Joel D. Rubenstein, MD • Jae K. Kim, SB, SM • Izabella Morava-Protzner, MD, PhD
Peter L. Stanchev, PhD • R. Mark Henkelman, PhD

Effects of Collagen Orientation on MR Imaging Characteristics of Bovine Articular Cartilage[1]

To determine the influence of collagen orientation on the magnetic resonance (MR) imaging appearance of articular cartilage, spin-echo MR images of normal bovine patellar specimens were obtained with the specimen rotated in 5° increments between +75° and −130°. Hyperintense superficial, hypointense middle, and intermediate-intensity deep laminae were observed. Results of polarized light microscopy of histologic specimens confirmed the three zones, and transmission electron microscopy showed different collagen arrangements in the zones. An anisotropic effect of rotation on signal intensity was evident, especially in the hypointense second lamina. Because of the preferential alignment of water molecules associated with collagen, angular rotation of the cartilage in the direction of minimum dipolar coupling (55° to the magnetic field) caused the cartilage to have a homogeneous appearance. The MR imaging appearance of these layers is strongly influenced by an anisotropic arrangement of the collagen fibers and by the alignment of the specimen relative to the magnetic field.

Index terms: Cartilage, MR, 4521.121411 • Joints, MR, 452.121411 • Magnetic resonance (MR), experimental • Magnetic resonance (MR), tissue characterization, 4521.121411

Radiology 1993; 188:219–226

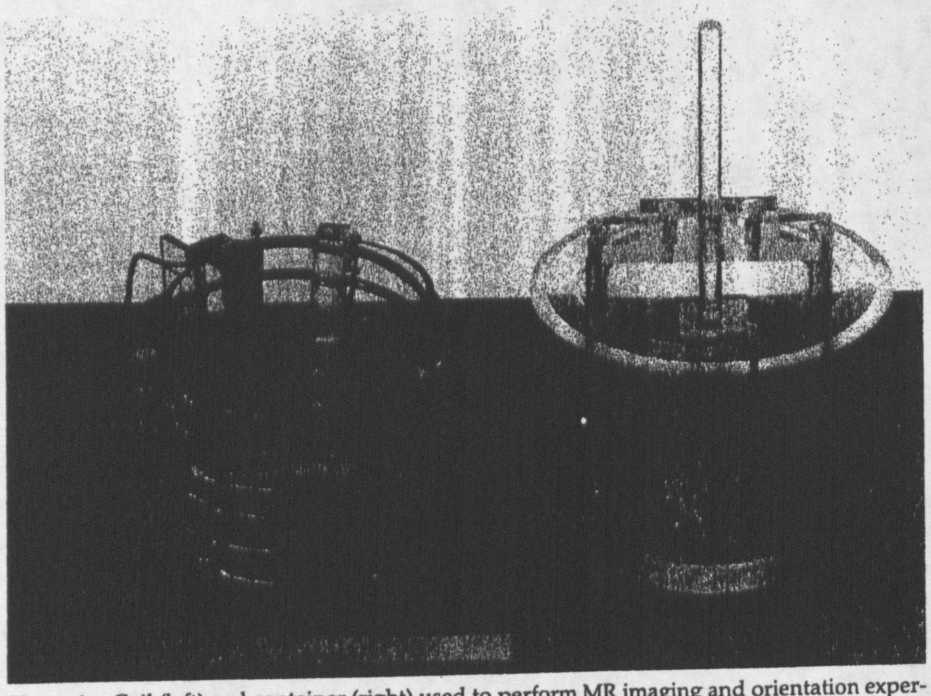

Figure 1. Coil (left) and container (right) used to perform MR imaging and orientation experiments. A patellar specimen is mounted in the container. For MR imaging, the container is placed within the bore of the upright radio-frequency coil. The apparatus design permits rotation of the coil around the vertical axis of the container within the coil. Accurate angular rotational measurements can be made by using the goniometer attached to the rim of the container.

In recent years, there have been numerous studies evaluating articular cartilage with magnetic resonance (MR) imaging (1–19). Most of these studies have examined the appearance of abnormal cartilage at MR imaging (1–16), while only a few have specifically examined the MR imaging appearance of normal articular cartilage (17–19). With excised bovine (17) or human cartilage (18,19), studies have shown that normal cartilage has a laminated appearance on MR images, although the findings differ with regard to the number, apparent thickness, and signal intensity characteristics of the laminae. In addition, there is as yet no satisfactory biophysical explanation for the appearance of the laminae.

The purpose of this investigation was to study excised normal bovine articular cartilage with MR imaging to assess the influence of collagen on the MR imaging appearance of cartilage. We hypothesized that the internal collagen structure of cartilage and its orientation strongly influence the appearance of the laminations through an anisotropic effect. Thus, MR images of cartilage were examined for orientation-dependent signal intensity variation such as that previously shown for MR images of tendons (20–22), and the relative direction of the collagen fibers in the cartilage was determined with polarized light microscopy and transmission electron microscopy and correlated with MR

Abbreviation: B_0 = constant magnetic induction field.

[1] From the Departments of Radiology (J.D.R., R.M.H.), Medical Biophysics (J.K.K., P.L.S., R.M.H.), and Pathology (I.M.P.), Sunnybrook Health Sciences Center, University of Toronto, 2075 Bayview Ave, Toronto, Ontario, Canada M4N 3M5. Received December 14, 1992; revision requested January 13, 1993; revision received January 29; accepted February 17. Supported by grant no. RP 2031 from the Sterling-Winthrop Imaging Research Institute. J.K.K. supported by a studentship from the Medical Research Council of Canada. **Address reprint requests to** J.D.R.

© RSNA, 1993

See also the editorial by Erickson et al (pp 23–25) in this issue.

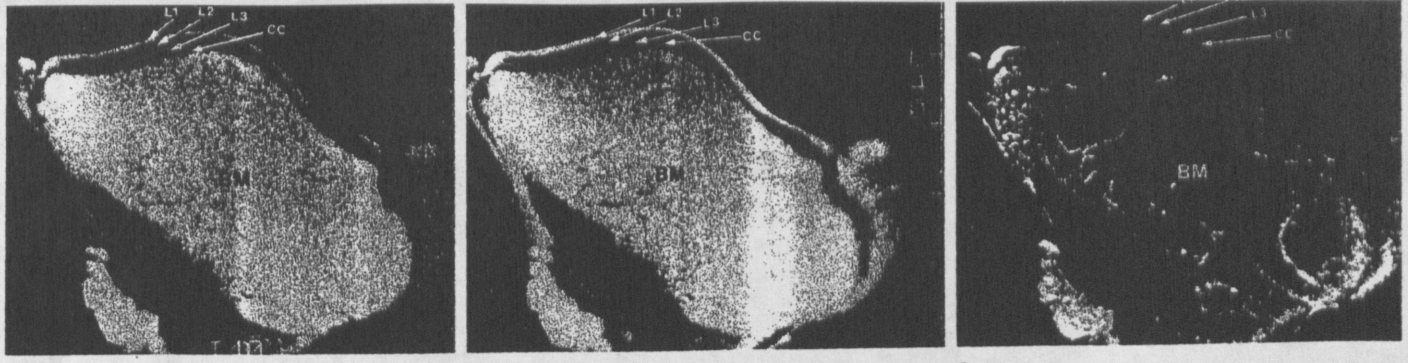

a. b. c.

Figure 2. *L1* = lamina 1, *L2* = lamina 2, *L3* = lamina 3, *CC* = calcified cartilage, *BM* = bone marrow. **(a)** T1-weighted (300/20), **(b)** proton-density–weighted (2,000/20), and **(c)** T2-weighted (2,000/70) axial images of the same section from a patellar specimen, with B_0 directed toward the top of the images, frequency encoding from top to bottom, and phase encoding from left to right. The three cartilage laminae are clearly seen, except in the T2-weighted image, which has a low signal-to-noise ratio. The nonuniform background mottle is due to photographic technique used to define the laminae for the illustrations. A scale in centimeters is on the right side of **b**.

imaging and conventional histologic findings.

MATERIALS AND METHODS

Articular cartilage from normal bovine patellae was used in this investigation. Eighteen fresh intact bovine knees were obtained from animals under 2 years of age and were frozen at −30°C. Prior to examination, each intact knee was thawed in a refrigerated compartment (44°C) for 48 hours and then kept at room temperature for 6 hours. The patella was dissected free from the intact knee and attached soft tissues immediately prior to MR imaging.

A 12-cm-diameter transmit-receive solenoidal radio-frequency coil was constructed. The coil incorporated a separate polymethyl methacrylate receptacle for specimen mounting, to provide rigid fixation of the patella and accurate rotational measurements (Fig 1). The specimen was mounted such that the planar surface of the cartilage was perpendicular to the base of the container, to minimize partial volume averaging of the signal from the cartilage laminae. To maintain the humidity within the container during the imaging experiments, a small volume of water was placed in the base of the container, and the top of the container was covered with moist paper towels.

MR imaging was performed with a 1.5-T system (Signa 4.7; GE Medical Systems, Milwaukee, Wis). T1-weighted (300/20) (repetition time msec/echo time msec) and proton-density– and T2-weighted (2,000/20,70) images were obtained by using a 256 × 256 matrix, 8-cm field of view, two signals averaged, and 3.0-mm section thickness with a 1.5-mm intersection gap.

Initial assessment of the cartilage laminae was performed with T1-, proton-density–, and T2-weighted imaging sequences. Axial images were obtained with the planar surface of the cartilage facing the direction of B_0, such that the frequency-encoding direction was anteroposterior and the phase-encoding direction was left to right. Detail of the cartilage laminae was best seen on the T1-weighted and proton-density–weighted images. Although the laminar appearance was similar on the T2-weighted images, the signal-to-noise ratio was inadequate for clear definition of the laminae. Thus, T1-weighted sequences were used for the angular dependence experiments.

For the experiments in which anisotropic effects were studied, images through the axial plane of the intact patellar specimens were obtained with specimen rotation about the vertical axis in 5° increments between +75° and −130°. The 0° position was referenced with the region of interest of the articular surface of the cartilage on the lateral patellar facet perpendicular to the constant magnetic induction field (B_0). Additional images were obtained at 0°, 180°, −90°, and +90° specifically to check for chemical shift effects on the acquired images, although this effect could alternatively have been assessed by swapping the phase and frequency directions.

Signal intensity profiles of the cartilage laminae were obtained from the MR images at each increment of rotation. Computer software was used to first rerotate each acquired image the number of degrees needed to return the specimen to the 0° orientation. Signal intensity versus

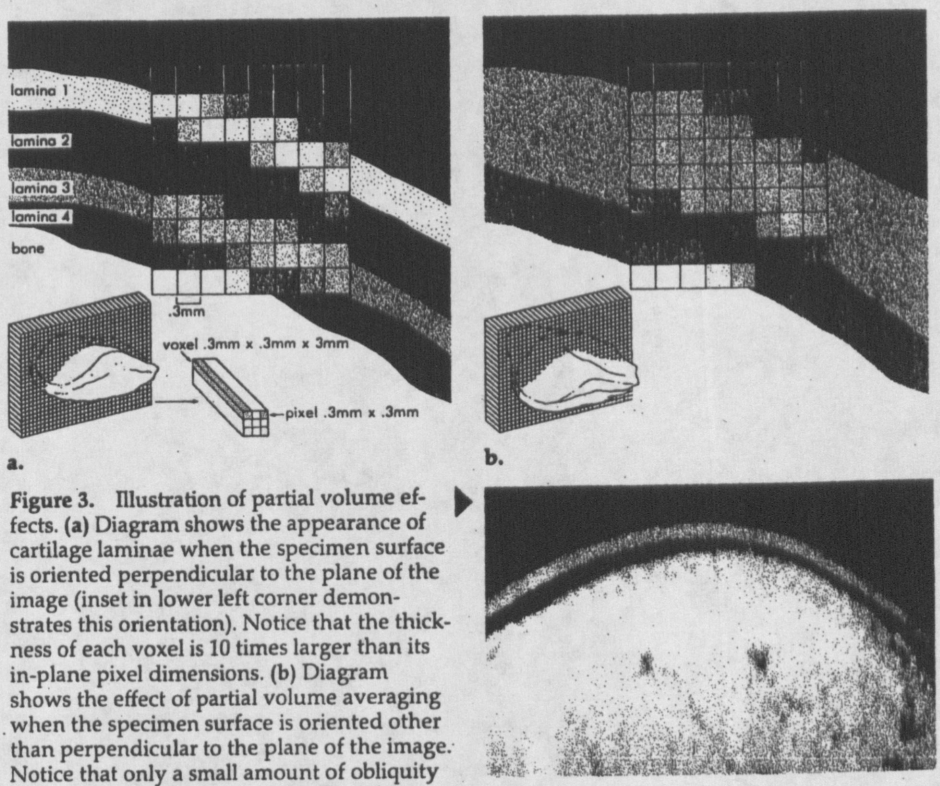

a. b. c.

Figure 3. Illustration of partial volume effects. **(a)** Diagram shows the appearance of cartilage laminae when the specimen surface is oriented perpendicular to the plane of the image (inset in lower left corner demonstrates this orientation). Notice that the thickness of each voxel is 10 times larger than its in-plane pixel dimensions. **(b)** Diagram shows the effect of partial volume averaging when the specimen surface is oriented other than perpendicular to the plane of the image. Notice that only a small amount of obliquity is necessary to obliterate the laminae, because of the elongated voxel dimensions. **(c)** Axial MR image (300/20). Appearance of the cartilage with the articular surface not perpendicular to the plane of the image. Notice the homogeneous signal intensity of the cartilage and lack of visible laminae.

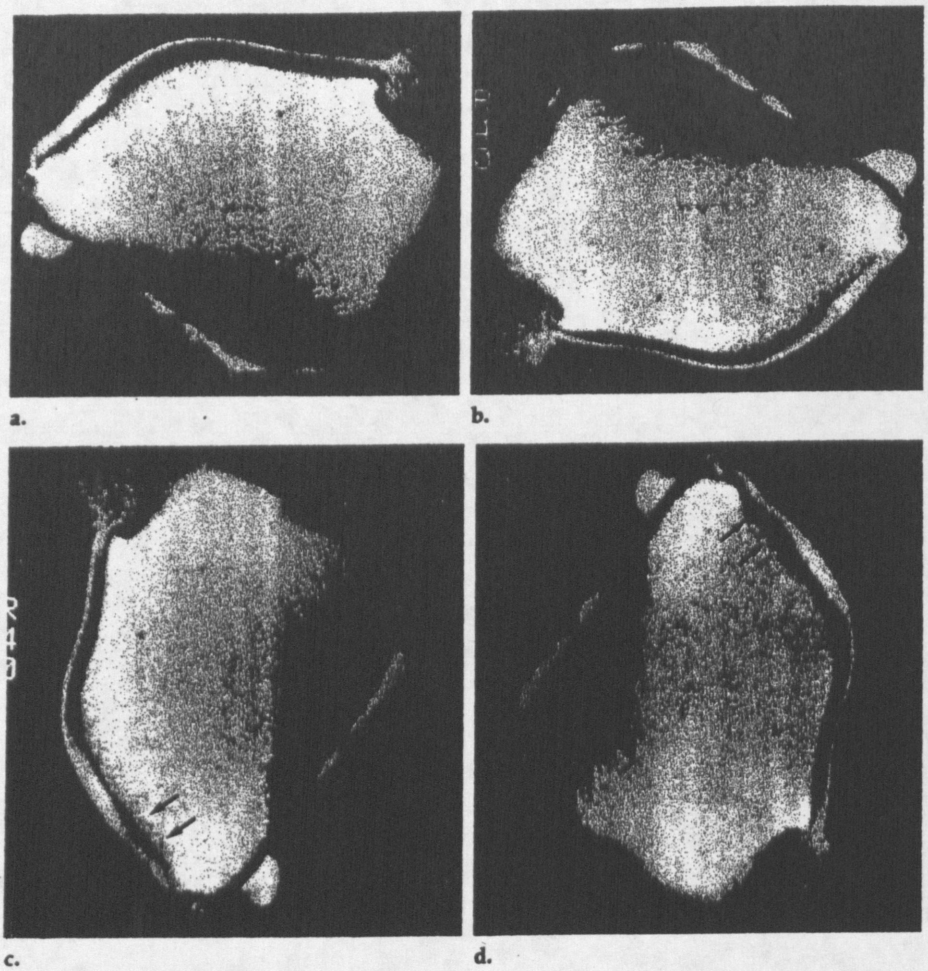

Figure 4. Chemical shift is seen at the junction of cartilage and bone marrow on T1-weighted images (300/20) obtained with B_0 directed toward the top of the images and the frequency-encoding direction oriented from top to bottom. (a) Lamina 3 and the lamina of calcified cartilage are clearly visible at 0°, but (b) have disappeared with the specimen rotated 180°. The same section viewed at (c) −90° and (d) +90°, in the phase-encoding direction, shows that the images are identical, except for slight chemical shift in the margins of the specimen (arrows in c, d) that are facing the frequency-encoding direction (see Fig 6).

cartilage depth was then plotted for the cartilage segments in each rerotated image by summing the signal intensity of 20 adjacent pixels parallel to the cartilage surface at each depth. By using the same data, the average signal intensity from each distinct lamina was obtained and plotted against the angle of rotation to assess the orientation dependence of the signal intensity from each lamina.

The computerized rotation scheme used a simple interpolation rotation algorithm around the center of rotation of the patellar specimen. The center of rotation of the specimen was determined by removing the specimen from the container at the end of a rotation series and filling the container with "doped" water (1 mL of gadolinium in 1,000 mL of saline solution); images perpendicular to the cylindric axis of the container then provided an outline of the container from which the center could easily be determined.

After MR imaging, corresponding sections of the cartilage were prepared for examination with routine light microscopy, polarized light microscopy, and transmission electron microscopy. The specimens were first fixed in 10% neutral formalin. Hultkrantz split lines were then created by using a small pin and were enhanced by using Davidson marking ink (Bradley Products, Bloomington, Minn) (23). The central portion (1–1.2 cm) of the patella was sectioned horizontally into 3–4-mm-thick slices to correspond to the plane of the MR images. The slices were then decalcified with a mixture of equal volumes of 50% formic acid and 20% sodium citrate solutions.

For light microscopy, one or two slices containing the articular cartilage were blocked, processed routinely, and embedded in paraffin. The paraffin sections (5-μm thick) were stained with hematoxylin and eosin.

For transmission electron microscopy, small blocks were prepared from the remaining specimen slices. These were cut perpendicular to the articular surface and parallel to a split line. The blocks were processed for embedding in plastic. The marking ink was used to assist proper orientation of the sample at embedding. Thin (0.1-μm) sections were stained with uranyl acetate and lead citrate and examined by means of transmission electron microscopy (EM109; Carl Zeiss, Thornwood, NY). The cartilage was studied through its entire depth, and the orientation of the collagen fibers was noted at each depth.

RESULTS

In the following results and discussion, the word lamina is used to refer to a specific stratum of cartilage seen with MR imaging, and the word layer is used to refer to a stratum of cartilage seen at histologic evaluation.

Each of the T1-, proton-density–, and T2-weighted axial images in the initial assessment showed three laminae (Fig 2), consisting of a superficial lamina of hyperintense signal (lamina 1), a middle lamina of hypointense signal (lamina 2), and a deep lamina of intermediate signal intensity (lamina 3). A distinct fourth lamina of hypointense signal, which subsequently proved to represent the calcified cartilage and cortical bone, separated the three cartilage laminae from the hyperintense signal intensity of the bone marrow.

Partial Volume and Chemical Shift Effects

If the planar surface of the cartilage was not carefully oriented to be perpendicular to the imaging plane, the cartilage had a homogeneous appearance, caused by partial volume effects through the 3-mm section thickness of the 0.3 × 0.3-mm² pixels (Fig 3).

The orientation experiments showed that chemical shift affected the number of apparent laminae on the MR images (Fig 4). Comparison of the cartilage appearance in the 0° and 180° orientations (frequency encoding was bottom to top) showed that the marrow signal intensity obscured the intermediate signal intensity of lamina 3 and the low signal intensity from the calcified cartilage to give the appearance of only two laminae at 180° and also caused an increase in the apparent thickness of low-signal-intensity calcified cartilage at 0°. Profiles obtained at the −90° and +90° positions (corresponding to the phase-encoding direction and therefore not subject to chemical shift artifact) confirmed the true presence and thickness of lamina 3 and the hypointense lamina of calcified cartilage.

Orientation Effects

Qualitative analysis of the angular orientation experiments showed that the trilaminar appearance of the cartilage was most apparent along the portions of the articular surface facing

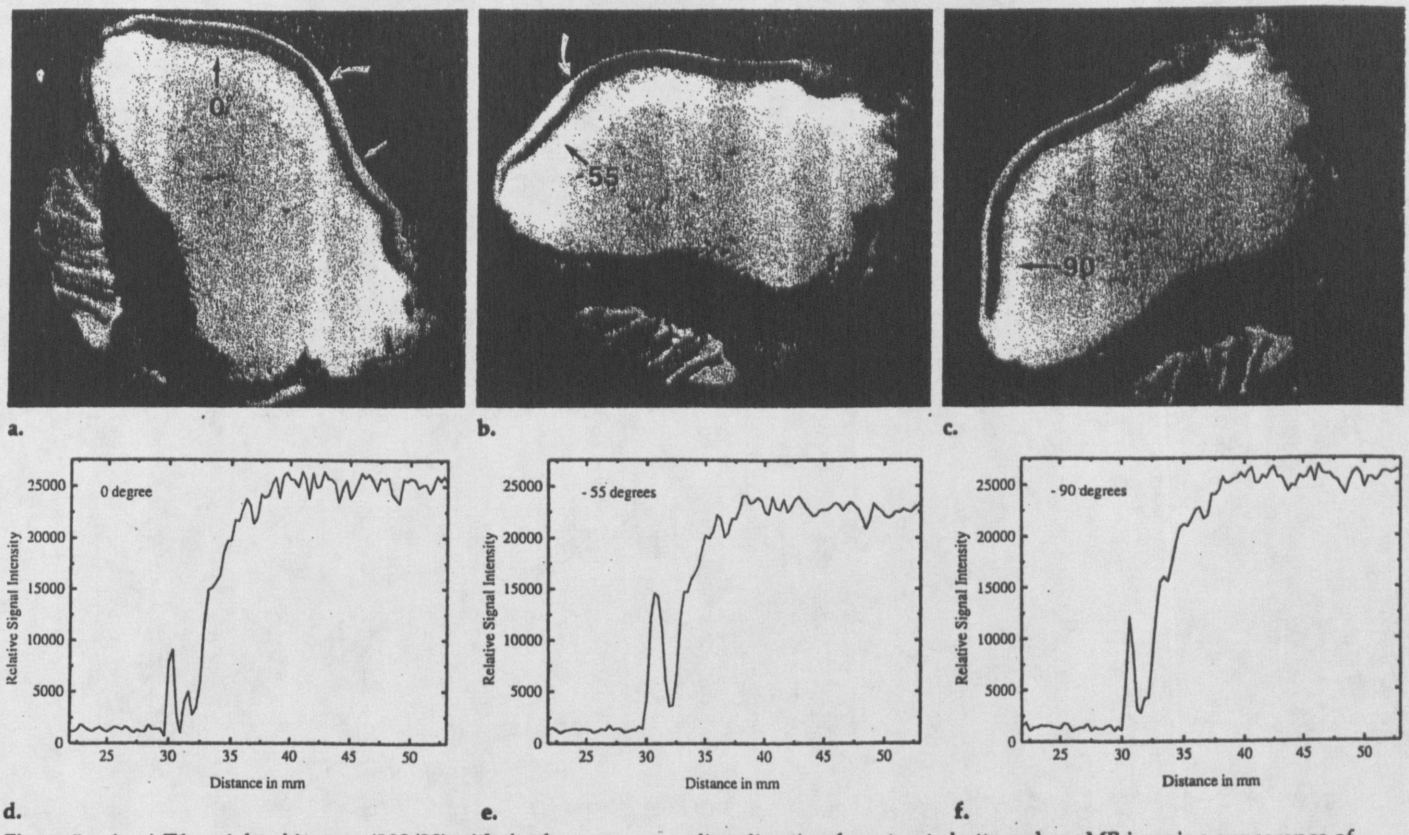

Figure 5. (a–c) T1-weighted images (300/20) with the frequency-encoding direction from top to bottom show MR imaging appearance of cartilage laminae at (a) 0°, (b) −55°, and (c) −90° of rotation (black arrows) relative to B_0, which is directed toward the top of the illustrations. (d–f) Corresponding signal intensity profiles at (d) 0°, (e) −55°, and (f) −90°. The signal intensity profile begins at the left in air, and the level reflects the image noise. The surface of the cartilage starts at 30 mm and, crossing the cartilage laminae, is into the bone marrow at 35 mm and beyond. Three laminae are visible when the cartilage faces 0° and −90°, but the middle hypointense lamina becomes hyperintense when the cartilage faces the −55° direction. The transition point where the "magic angle" effect is most evident occurs between the lateral and medial facets (curved arrow in a, b). The hyperintense middle lamina can also be seen when the cartilage faces +55° (straight white arrow in a).

the 0° and −90° positions (Fig 5a–5c). The signal intensity of lamina 2 showed dramatic variation with rotation; minimum signal intensities were present at the 0° and −90° orientations, with a maximum signal intensity in between. In these oblique orientations, the cartilage appeared homogeneous through the three layers. The signal intensities of lamina 1 and lamina 3 did not visibly change with orientation, although quantitative measurements show that the intensity of lamina 1 approximately doubled between 0° and −55° (Fig 5d–5f).

Quantitative analysis of the results from the orientation experiments confirmed the anisotropy observed at visual inspection of the images included as Figure 4. For each angular orientation, the average signal intensity in the first two pixels below the articular surface of the cartilage (lamina 1), the next two pixels (lamina 2), and the fifth and sixth pixels (lamina 3) were plotted (Fig 6). The signal intensity versus rotation angle plots confirm that, with rotation, the signal intensity of lamina 2 changed to a greater degree than the others. Less pronounced anisotropic behavior was noticed in the signal intensity of lamina 1, which had absolute peak signal intensities at −55° and +55° that were greater than those in lamina 2 but a smaller percentage variation between the base and peak values (80% for lamina 1 versus 330% for lamina 2). Unlike the signal intensity from laminae 1 and 2, the signal intensity from lamina 3 remained constant with rotation angle. At angles between −130° and −110°, the chemical shift artifact (Fig 4a, 4b) causes intrusion of the marrow signal intensity into lamina 3, resulting in a small increase in signal intensity.

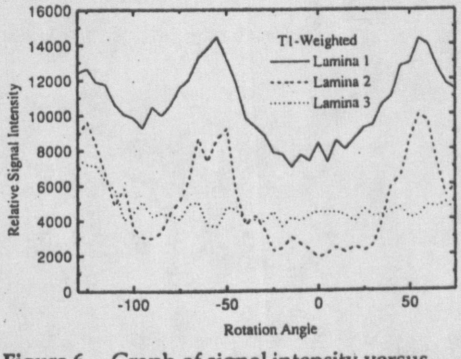

Figure 6. Graph of signal intensity versus rotation angle. The signal intensity of lamina 2 shows well-defined peaks at +55°, −55°, and −125°. Lamina 1 also has signal intensity peaks due to radially oriented fibers. The rise in signal intensity of lamina 3 between −110° and −130° is due to chemical shift.

Light Microscopic Findings

The histologic sections of the cartilage specimens examined with polarized light microscopy showed a layered appearance that was not apparent with routine light microscopy (Fig 7). A superficial dark layer (0.35 mm ± 0.15) was seen with polarized light microscopy, representing the tangential and transitional zones, and a thin bright line (0.02–0.04-mm thick) was noted at the articular surface of this superficial dark layer. Lower than the superficial dark layer, a wide bright layer (0.85 mm ± 0.25) was seen, representing the upper two-thirds of the radial zone. Next, a narrow dark layer (0.30 mm ± 0.20) was located in the lower third of the radial zone. The deepest layer (0.50 mm ± 0.20) was bright at polarized light microscopy and included the deepest portion of the unmineralized

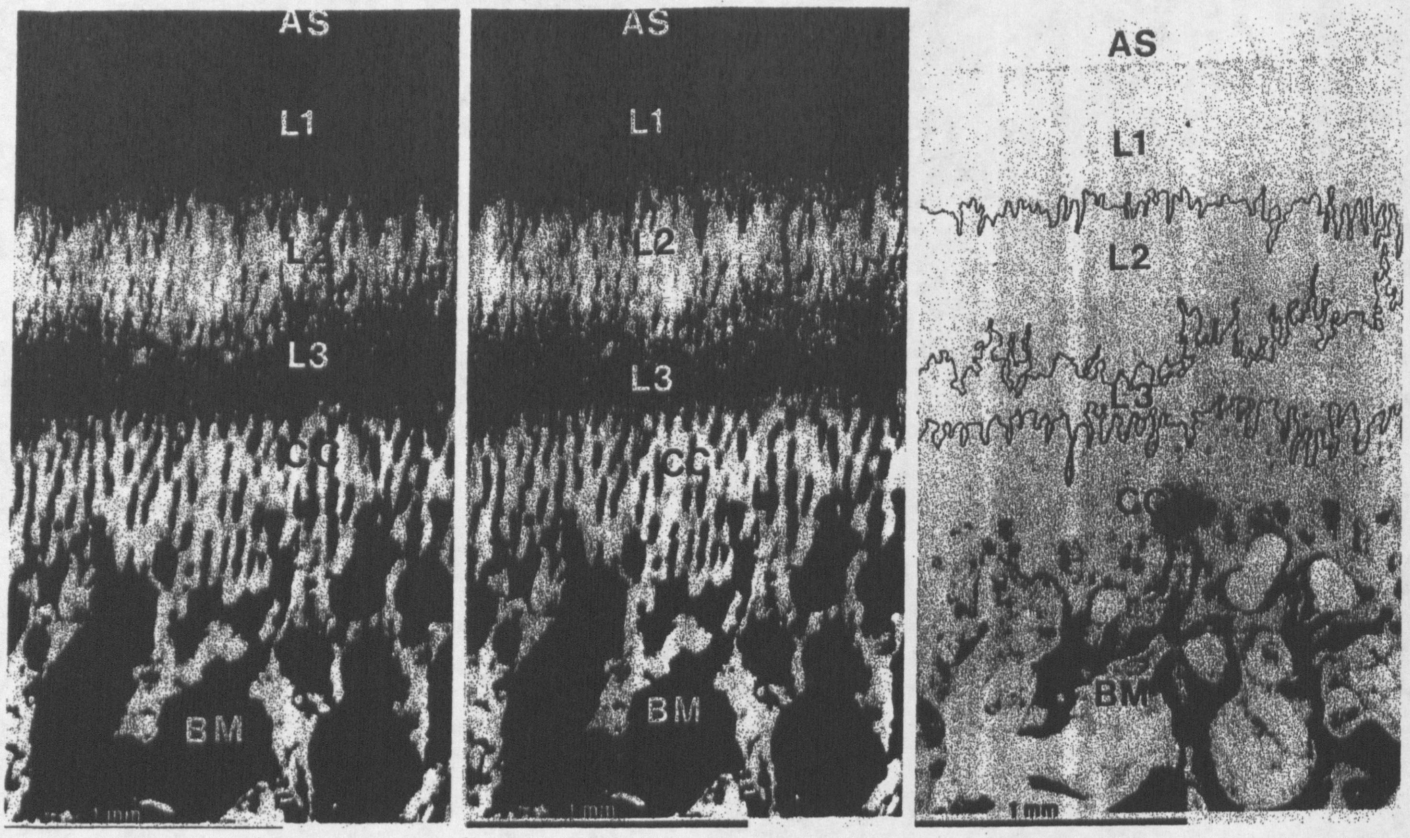

a. b. c.

Figure 7. *AS* = articular surface, *L1* = layer 1, *L2* = layer 2, *L3* = layer 3, *CC* = calcified cartilage, *BM* = bone marrow. **(a)** Hematoxylin and eosin-stained section of the articular cartilage examined with polarized light microscopy. Four distinct layers are seen with polarized light. (Original magnification, ×60.) **(b)** Computerized image analysis of a shows lines defining irregular undulating transition between laminae. **(c)** Routine light microscopy of same section of articular cartilage, with lines of transition from **b** superimposed to show location of laminae that are otherwise not visible (original magnification, ×60).

radial zone of cartilage, the tidemark, and the calcified cartilage. Beneath this bright layer was the combination of bright bony trabeculae and dark marrow spaces.

Electron Microscopic Findings

Ultrastructural examination with transmission electron microscopy was used to determine the collagen arrangement in the different zones of the articular cartilage (Fig 8), which was then correlated with the polarized light microscopic findings and the MR images. In the tangential zone, the fibers were arranged parallel to the articular surface (Fig 8a). In the transitional zone, fibers were seen running parallel, oblique, and perpendicular to the articular surface, gradually changing with depth (ie, fiber arrangement was predominantly parallel to the articular surface in the upper part of this zone but became mostly perpendicular in its lower portion) (Fig 8b). In the upper two-thirds of the radial zone, the fibers were aligned perpendicular to the articular surface (Fig 8c); in the lower third of the radial zone, this highly regular perpendicular arrangement of fibers was distorted (Fig 8d). Just above the tidemark (Fig 8e), the strict perpendicular arrangement returned.

DISCUSSION

Bovine (17) and human (18,19) cartilage have been the subject of a limited number of studies attempting to characterize normal articular cartilage with MR imaging. Although each of these studies has shown that normal cartilage has a laminated appearance on MR images, they have nonetheless presented conflicting results about the number and nature of the laminae.

With fresh bovine patellae, Lehner et al were among the first to study the structure of articular cartilage with MR imaging. They identified two laminae (17). On T1-weighted inversion recovery and T2-weighted spin-echo images, the cartilage was observed to have a bilaminar appearance, with a superficial lamina with long T1 and T2 and a deep lamina with short T1 and T2. Also, the cartilage appeared homogeneous on proton-density– and T1-weighted spin-echo images, as well as on gradient-echo images. Lehner et al also attempted to correlate the cartilage laminae seen on MR images with histologic layers identified microscopically and concluded that the superficial lamina corresponded with the histologic tangential and transitional zones while the deep lamina represented the histologic radial zone. The authors ultimately attributed the differences in signal intensity characteristics between the two laminae strictly to the zonal variation in water content.

Hayes et al (18), in a correlative study of patellar cartilage lesions from 14 human knees, noted that on T1-weighted images, normal cartilage showed either homogeneous intermediate signal intensity or a bilaminar appearance with a thin, high-signal-intensity superficial lamina and a low-intensity deep lamina, but they did not attempt to explain why the appearance of normal cartilage varied between homogeneous and bilaminar.

In an assessment of the knee and ankle joints of a single human cadaver with high-resolution MR imaging, Modl et al (19) found three zones

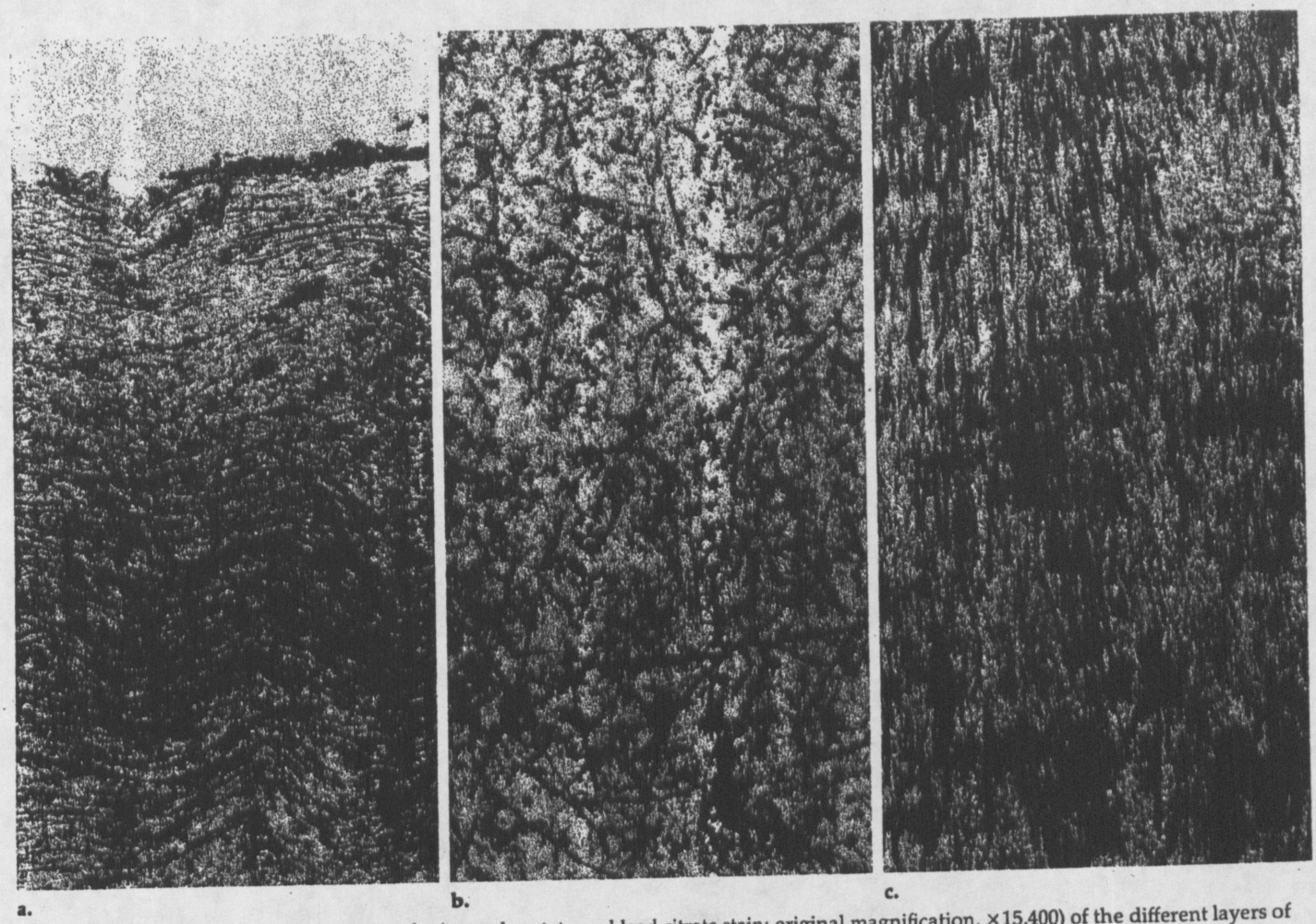

Figure 8. Transmission electron micrographs (uranyl acetate and lead citrate stain; original magnification, ×15,400) of the different layers of the articular cartilage, showing arrangement of the collagen fibers relative to the articular surface: **(a)** In the tangential zone, the fibers are parallel to the articular surface; **(b)** in the transitional zone, fibers are aligned parallel, oblique, and perpendicular; **(c)** in the upper radial zone, the fibers are perpendicular. *(Fig 8 continues).*

of different signal intensity in the articular cartilage and attempted to correlate this observation with the histologic zones of normal cartilage. Specifically, they identified a narrow band of low signal intensity at the articular surface, which they related to the tangentially oriented collagen fibers seen histologically; a middle zone of higher signal intensity, correlating with the transitional zone of cartilage; and a deep, low-signal-intensity zone representing the radial and calcified cartilage plus cortical bone. These investigators stated, however, that the superficial low-intensity zone seen with MR imaging corresponded in location, but not in thickness, to the superficial histologic zone, and that the other two laminae showed only an approximate correlation. Moreover, they were unable to explain what determined the signal intensity characteristics in the different zones of the cartilage, although they suggested that the magnetic susceptibility of collagen fibers oriented in different directions might be one explanation.

In contrast to Modl et al's suggestion of a susceptibility effect, we believe that the orientation-dependent T2 of collagen fibers is a more critical determinant of the signal intensity from the various cartilage laminae. In 1962, Berendsen first described the anisotropic effect of collagen fibers for partially hydrated bovine Achilles tendon (20). He attributed this property to the anisotropic motion of water molecules parallel to the direction of collagen fibers. Spin-spin coupling (T2) between two adjacent protons is mediated by the respective magnetic dipolar fields of each proton. The magnetic dipolar fields are characterized by the term $(3\cos^2\theta - 1)$, where θ is the angle between B_0 and a vector through adjacent protons (20–22). In the case of freely moving water protons, this angular dependence averages to zero; with the angular anisotropy of water molecules along the collagen fibers, however, a net angular dependence remains, leading to an anisotropic T2. With this anisotropy, spin-spin coupling is minimized (ie, T2 is maximal) at the angle where $(3\cos^2\theta - 1) = 0$; this corresponds to $\theta = 55°$, which is also known as the magic angle.

Subsequent studies by Peto and Gillis (21) and Fullerton et al (22) have shown that this phenomenon occurs even with full hydration of the tendon, while in vivo MR imaging studies have also shown this behavior in human tendon (24). Thus, human and animal tendons, which contain large amounts of collagen fibers oriented in a single predominant direction, show the anisotropic T2 properties of collagen fibers. Our investigation has shown that this anisotropic T2 effect of collagen can be seen in tissues other than tendon, even though tissues such as cartilage contain smaller amounts of collagen fibers. Moreover, we have shown that the signal intensity from each of the cartilage laminae has a different angular dependence.

Since the signal intensity from collagen fibers is characteristic of the orientation of those fibers relative to B_0, inferences can be made about the angular dependence of each cartilage lamina seen on MR images and the

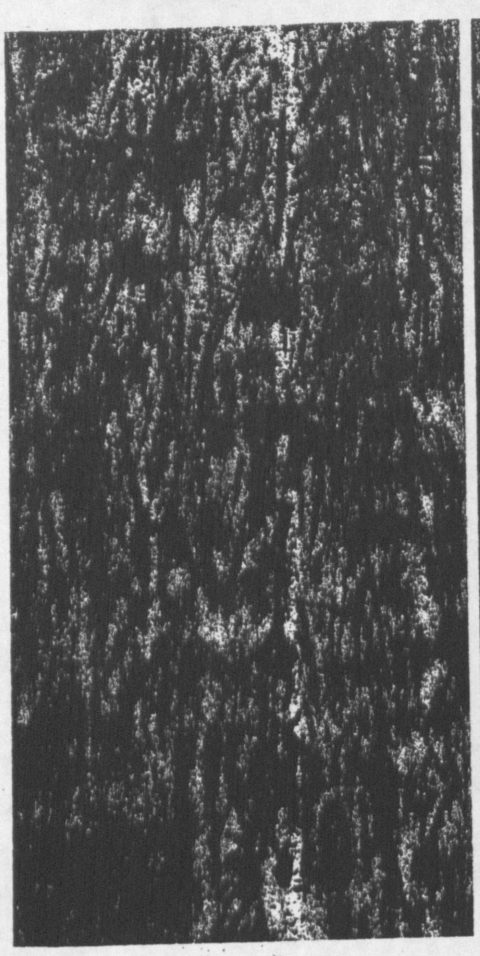

d.

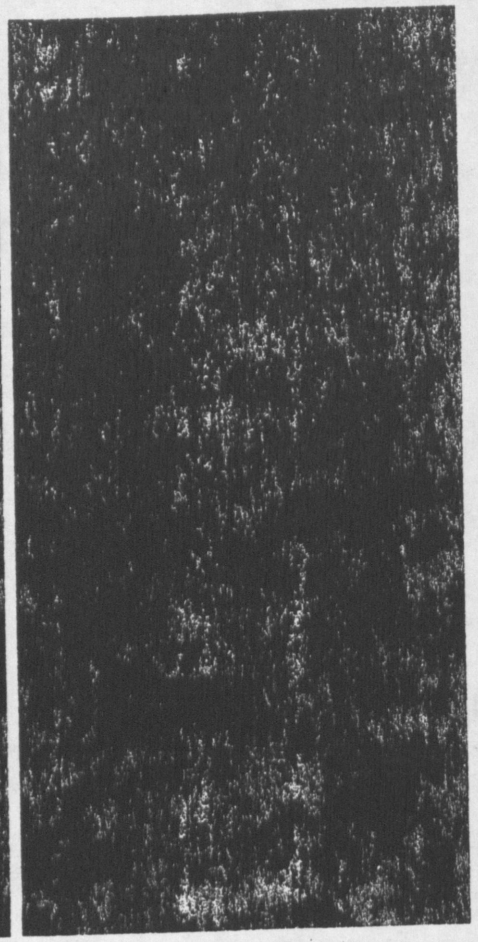

e.

Figure 8 *(continued).* **(d)** In the lower radial zone, numerous curved fibers are seen in addition to the perpendicular fibers. **(e)** In the zone of the tidemark, the fibers are densely packed and again perpendicular to the articular surface.

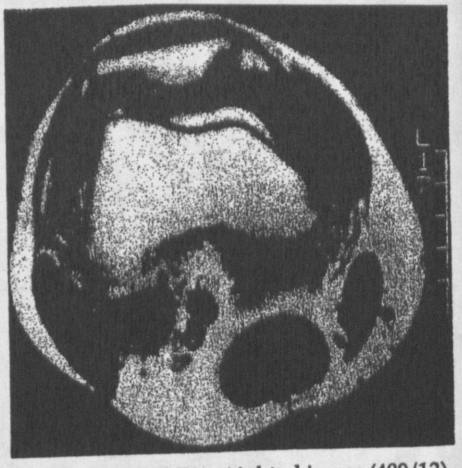

Figure 9. Axial T1-weighted image (400/12) of the knee of a patient with a joint effusion. Notice that the cartilage of the lateral patellar facet shows a trilaminar appearance of superficial hyperintense signal, intermediate hypointense signal, and deep hyperintense signal. Frequency encoding is from top to bottom, and phase encoding is from left to right.

predominant orientation of collagen fibers that contribute to their signal intensity. For example, in lamina 2, the peaks of signal intensity at −55° and +55° reflect the influence of collagen fibers that are oriented radially to the cartilage surface and obliquely to B_0. Although there was less anisotropy observed in lamina 1 than lamina 2, the peaks of the signal intensity at −55° and +55° in lamina 1 also reflect the strong influence of radially oriented collagen fibers.

It was also noted that the base level as well as the peak levels of signal intensity from lamina 1 were higher than those from lamina 2, which we believe may reflect the greater concentration of water in the superficial regions of the cartilage than in the deeper regions (25,26).

The explanation for the presence of lamina 3 and its lack of anisotropic behavior is not obvious, although we speculate that it could be related to the relative lack of a predominant fiber orientation resulting from the distortion of the collagen arrangement seen at transmission electron microscopy.

Knowledge of the collagen structure in articular cartilage is thus crucial to understanding the different angular dependence of each lamina at MR imaging. Early work by Hultkrantz (23) and later studies by Benninghoff, with polarized light microscopy (27,28), were instrumental in defining the specific arrangement of collagen in cartilage. An important characteristic of collagen is that its oriented, elongated fibers show form (or textural) birefringence when examined with polarized light (29). On the basis of collagen arrangement, Benninghoff described four relatively distinct zones in articular cartilage (28): a superficial tangential zone (zone 1), where the collagen fibers are horizontally arranged parallel to the articular surface; a middle transitional zone (zone 2), where collagen fibers are oriented obliquely to the articular surface; a deep radial zone (zone 3), in which the collagen fibers run vertically toward the surface; and the calcified cartilage zone (zone 4), located between the radial zone and the marrow.

Subsequent reports have emphasized that the orientational structure of articular cartilage is not apparent with light microscopy performed with conventional staining methods, but that polarized light microscopy reveals the pattern of collagen fibers in the cartilage and that electron microscopy can be used to define the arrangement of the individual collagen fibrils (30–32).

More recently, the three-dimensional architecture of collagen in bovine articular cartilage has been defined by using scanning electron microscopy of cryofractured specimens (33). The collagen fibrils are vertically oriented in the intermediate zone and curve to become horizontal in the superficial zone, where they are parallel to the articular surface. Of additional importance is the observation that the collagen structure is anisotropic, such that the collagen is organized in broad flat layers or leaves when viewed parallel to a split line, but when visualized at right angles to a split line, it has a vertically laminated appearance, as if the leaves are being viewed edge on.

We have used the results of these histologic studies to define the relationship between the collagen fiber arrangement in articular cartilage and the resultant MR imaging appearance of the cartilage, although it should be appreciated that certain factors prevent an exact correlation between the MR imaging laminae and the histologic zones. Specifically, in-plane voxel dimensions (0.3 × 0.3 mm) were too large to accurately resolve each histologic layer, which led to signal

averaging from different histologic layers. Furthermore, the junctions between the histologic zones undulate and do not have sharply defined interfaces.

Even with these limitations, we believe there are approximate correlations between the laminae visible on MR images and the histologic layers. Lamina 1 corresponds approximately to the histologic tangential and transitional zones, plus the upper portion of the radial zone, such that about half of lamina 1 is composed of the radial zone. This correlation agrees well with the evidence from the angular dependence experiments indicating the presence of both radial and perpendicular fibers.

Approximate correlations also exist between lamina 2 and the bulk of the radial zone (which supports the inference of radially oriented fibers in lamina 2, from the results of the angular dependence experiments) and between lamina 3 and the lower portion of the radial zone. Finally, the low-signal-intensity region separating lamina 3 from the marrow correlates with the zone of the tidemark and calcified cartilage.

We have shown that the MR imaging appearance of articular cartilage is strongly influenced by the anisotropic arrangement of the collagen fibers in the cartilage, particularly where the collagen orientation is radial, as in lamina 2. We have also shown that the MR imaging appearance of normal bovine cartilage consists of three laminae, yet the cartilage may appear homogeneous in signal intensity at certain orientations corresponding to the magic angle of 55°, or when the planar surface of the cartilage is not perpendicular to the imaging plane because of partial volume effects. Thus, orientation of the cartilage relative to B_0 is an important determinant for the MR imaging appearance of articular cartilage, although other factors may also be operative.

In conclusion, our findings are of potential clinical importance with regard to MR imaging of articular cartilage. In human beings, we have frequently identified a laminated appearance in the patellar cartilage on routine MR images of the knee (Fig 9), similar to that seen in bovine cartilage; therefore, the same principles affecting the MR imaging appearance of bovine cartilage can be expected to apply to human cartilage. Finally, an understanding of the orientation effects exhibited by normal articular cartilage combined with techniques that improve resolution (such as volume imaging) may serve as the basis for future studies of cartilage diseases. ■

Acknowledgments: We thank Kenneth P. H. Pritzker, MD, and Harpal K. Gahunia, MS, for their insights about the laminar appearance of articular cartilage at MR imaging, Howard I. Rosenberg, BSc, for assistance with the ultrastructural studies, Gordon Maxwell for supplying the bovine specimens, and Patsy Cunningham for artwork in Figure 3.

References

1. McCauley TR, Kier R, Lynch KJ, Jokl P. Chondromalacia patellae: diagnosis with MR imaging. AJR 1992; 158:101–105.
2. Monson NL, Haughton VM, Modl JM, Sether LA, Ho KC. Normal and degenerating articular cartilage: in vitro correlation of MR imaging and histologic findings. JMRI 1992; 2:41–45.
3. Chandnani VP, Ho C, Chu P, Trudell D, Resnick D. Knee hyaline cartilage evaluated with MR imaging: a cadaveric study involving multiple imaging sequences and intraarticular injection of gadolinium and saline solution. Radiology 1991; 178:557–561.
4. König H, Aicher K, Klose U, Saal J. Quantitative evaluation of hyaline cartilage disorders using flash sequence. I. Method and animal experiments. Acta Radiol 1990; 31:371–375.
5. König H, Aicher K, Klose U, Saal J. Quantitative evaluation of hyaline cartilage disorders using flash sequence. II. Clinical applications. Acta Radiol 1990; 31:376–381.
6. De Smet AA, Fisher DR, Graf BK, Lange RH. Osteochondritis dissecans of the knee: value of MR imaging in determining lesion stability and the presence of articular cartilage defects. AJR 1990; 155:549–553.
7. Handelberg F, Shahabpour M, Casteleyn PP. Chondral lesions of the patella evaluated with computed tomography, magnetic resonance imaging and arthroscopy. Arthroscopy 1990; 6:1–2.
8. Braunstein EM, Brandt KD, Albrecht M. MRI demonstration of hypertrophic articular cartilage repair in osteoarthritis. Skel Radiol 1990; 19:335–339.
9. Cole PR, Jasani MK, Wood B, Freemont AJ, Morris GA. High resolution, high field magnetic resonance imaging of joints: unexpected features in proton images of cartilage. Br J Radiol 1990; 63:907–909.
10. Karvonen RL, Negendank WG, Fraser SM, Mayes MD, An T, Fernandez-Madrid F. Articular cartilage defects of the knee: correlation between magnetic resonance imaging and gross pathology. Ann Rheum Dis 1990; 49:672–675.
11. Mink JH, Deutsch AL. Occult cartilage and bone injuries of the knee: detection, classification, and assessment with MR imaging. Radiology 1989; 170:823–829.
12. Yulish BS, Montanez J, Goodfellow DB, Bryan PJ, Mulopulos GP, Modic MT. Chondromalacia patellae: assessment with MR imaging. Radiology 1987; 164:763–766.
13. Gylys-Morin VM, Hajek PC, Sartoris DJ, Resnick D. Articular cartilage defects: detectability in cadaver knees with MR. AJR 1987; 148:1153–1157.
14. Sabiston CP, Adams ME, Li DKB. Magnetic resonance imaging of osteoarthritis: correlation with gross pathology using an experimental model. J Orthop Res 1987; 5:164–172.
15. Wojtys E, Wilson M, Buckwalter K, Braunstein E, Martel W. Magnetic resonance imaging of knee hyaline cartilage and intraarticular pathology. Am J Sports Med 1987; 15:455–463.
16. König H, Sauter R, Deimling M, Vogt M. Cartilage disorders: comparison of spin-echo, CHESS, and FLASH sequence MR images. Radiology 1987; 164:753–758.
17. Lehner KB, Rechl HP, Gmeinwieser JK, Heuck AF, Lukas HP, Kohl HP. Structure, function and degeneration of bovine hyaline cartilage: assessment with MR imaging in vitro. Radiology 1989; 170:495–499.
18. Hayes CW, Sawyer RW, Conway WF. Patellar cartilage lesions: in vitro detection and staging with MR imaging and pathologic correlation. Radiology 1990; 176:479–483.
19. Modl JM, Sether LA, Haughton VM, Kneeland JB. Articular cartilage: correlation of histologic zones with signal intensity at MR imaging. Radiology 1991; 181:853–855.
20. Berendsen HJC. Nuclear magnetic resonance study of collagen hydration. J Chem Phys 1962; 36:3297–3305.
21. Peto S, Gillis P. Fiber-to-field angle dependence of proton nuclear magnetic relaxation in collagen. Magn Reson Imaging 1990; 8:705–712.
22. Fullerton GD, Cameron IL, Ord VA. Orientation of tendons in the magnetic field and its effect on T2 relaxation times. Radiology 1985; 155:433–435.
23. Hultkrantz W. Über die spaltrichtungen der gelenkknorpel. Verh Anat Ges 1898; 12:248.
24. Erickson SJ, Cox IH, Hyde JS, Carrera GF, Strandt JA, Estkowski LD. Effect of tendon orientation on MR imaging signal intensity: a manifestation of the "magic angle" phenomenon. Radiology 1991; 181:389–392.
25. Mankin HJ, Thrasher AZ. Water content and binding in normal and osteoarthritic human cartilage. J Bone Joint Surg [Am] 1975; 57:76–80.
26. Kuettner KE, Aydelotte MB, Thonar EJMA. Articular cartilage matrix and structure: a minireview. J Rheumatol 1991; 18(Suppl 27): 46–48.
27. Benninghoff A. Über den funktionellen bau des knorpels. Verh Anatomisch Gesell 1922; 31:250–267.
28. Benninghoff A. Form und bau der gelenkknorpel in ihren beziehungen zur funktion. I. Die modellierenden und formerhaltenden faktoren des knorpelreliefs. Z Gesamte Anat 1925; 76:43–63.
29. Chayen J. Polarised light microscopy: principles and practice for the rheumatologist. Ann Rheum Dis 1983; 42(suppl):64–67.
30. Weiss C, Rosenberg L, Helfet AJ. An ultrastructural study of normal young adult human articular cartilage. J Bone Joint Surg [Am] 1968; 50:663–674.
31. Bullough P, Goodfellow J. The significance of fine structure of articular cartilage. J Bone Joint Surg [Br] 1968; 50:852–857.
32. Speer DP, Dahners L. The collagenous architecture of articular cartilage. Clin Orthop 1979; 139:267–275.
33. Jeffery AK, Blunn GW, Archer CW, Bentley G. Three-dimensional collagen architecture in bovine articular cartilage. J Bone Joint Surg [Br] 1991; 73:795–801.

(60.) * Rubenstein J., Kim J, Protzner I., Stanchev P., Henkelman R.M., "Effects of Collagen on MR Imaging Characteristics of Borine Articular Cartilage", ***Radiology***, No. 188, 1993, 219-226.